

Supramolecular Chemistry

Local Self-Assembly of Dissipative Structures Sustained by Substrate Diffusion

Haridas Kar, Lorenzo Goldin, Diego Frezzato, and Leonard J. Prins*

Abstract: The coupling between energy-consuming molecular processes and the macroscopic dimension plays an important role in nature and in the development of active matter. Here, we study the temporal evolution of a macroscopic system upon the local activation of a dissipative self-assembly process. Injection of surfactant molecules in a substrate-containing hydrogel results in the local substrate-templated formation of assemblies, which are catalysts for the conversion of substrate into waste. We show that the system develops into a macroscopic (pseudo-)non-equilibrium steady state (NESS) characterized by the local presence of energy-dissipating assemblies and persistent substrate and waste concentration gradients. For elevated substrate concentrations, this state can be maintained for more than 4 days. The studies reveal an interdependence between the dissipative assemblies and the concentration gradients: catalytic activity by the assemblies results in sustained concentration gradients and, vice versa, continuous diffusion of substrate to the assemblies stabilizes their size. The possibility to activate dissipative processes with spatial control and create long lasting non-equilibrium steady states enables dissipative structures to be studied in the space-time domain, which is of relevance for understanding biological systems and for the development of active matter.

Introduction

Inspired by the properties of living systems a strong interest exists in the development of synthetic active matter.^[1–3] Chemically fueled self-assembly aims at exploiting the chemical energy stored in thermodynamically activated molecules, so called chemical fuels, to drive self-assembly processes away from thermodynamic equilibrium.^[4–6] The archetypical biological example is microtubule formation which relies on the coupling between endergonic tubulin self-assembly and exergonic guanosine triphosphate (GTP)-hydrolysis.^[7–9] In recent years, many chemically fueled synthetic self-assembly processes have been reported and

properties expected for a non-equilibrium structure, such as dynamic instability^[10] and oscillatory behavior,^[11,12] have indeed been observed. Yet, the development of active matter requires that energy-consuming processes at the molecular level are transduced to the macroscopic level. The role of microtubules in shaping the cell and acting as ‘molecular tracks’ for intracellular transport indeed indicate that in nature chemically fueled self-assembly is closely connected to the spatial dimension. The notion that macroscopic GTP-concentration gradients play a key role in the search and capture of kinetochores by microtubules during cell division indicates that in nature non-equilibrium events at the molecular (microtubule formation) and macroscopic (concentration gradients) scale can even be interdependent.^[13,14] Within the context of synthetic chemically fueled self-assembly there has been relatively little exploration of the spatial dimension. Yet, initial observations that locally activated chemically fueled self-assembly processes can lead to new macroscopic phenomena such as pattern formation,^[11,15,16] active droplets,^[17,18] and dissipative adaptation,^[19] illustrate that an understanding of how local energy dissipating events affect the macroscopic surrounding and vice versa is essential for the development of synthetic active matter.^[20–22]

Here, we show that the local activation of a chemically fueled dissipative self-assembly process in a hydrogel matrix results in the development of a macroscopic non-equilibrium steady state (NESS)^[23] characterized by the presence of persistent substrate (fuel) and product (waste) concentration gradients and a non-homogeneous macroscopic distribution of energy dissipating assemblies. At elevated substrate concentrations the steady state can be maintained for more than 4 days. The studies reveal an interdependent relationship between the dissipative structures and the concentration gradients: catalytic activity by the assemblies results in sustained concentration gradients and, vice versa, continuous diffusion of substrate to the assemblies stabilizes their size.

Results and Discussion

Dissipative self-assembly. The system that is reported here has been developed based on two insights obtained from previous studies. Regarding the self-assembly of dissipative structures, we have shown that 2-hydroxypropyl *p*-nitrophenyl phosphate (HPNPP) templates the self-assembly of surfactants $C_{16}TACN \cdot Zn^{2+}$ (**1**, TACN: 1,4,7-triazacyclononane, Figure 1a).^[24] Importantly, assembly formation acti-

[*] Dr. H. Kar, L. Goldin, Dr. D. Frezzato, Prof. Dr. L. J. Prins
 Department of Chemical Sciences
 University of Padova
 Via Marzolo 1, 35131 Padova, Italy
 E-mail: leonard.prins@unipd.it

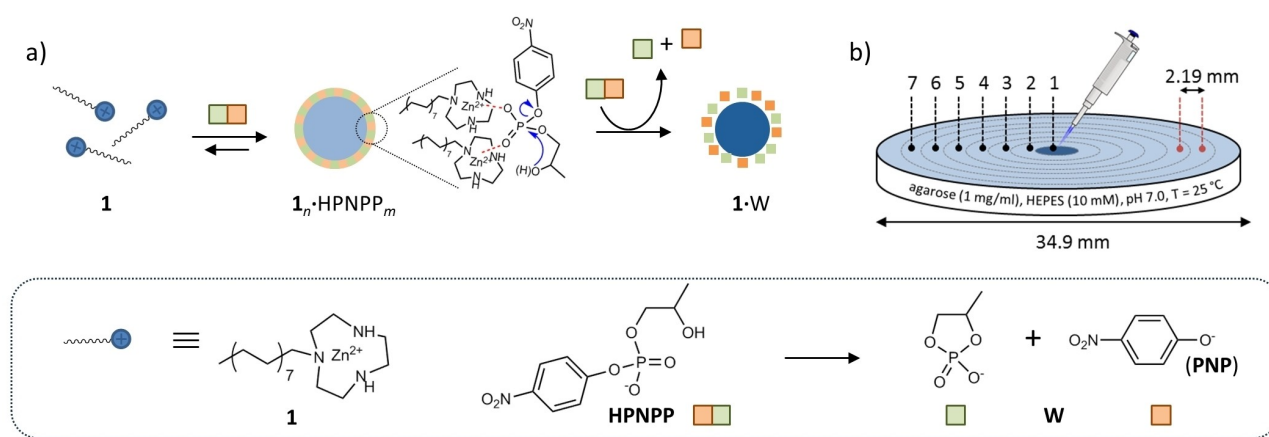


Figure 1. a) Schematic representation of the substrate-induced self-assembly of assemblies $1_n \cdot \text{HPNPP}_m$ that display cooperative catalysis in the cleavage of HPNPP leading to waste-stabilized assemblies $1 \cdot \text{W}$. b) Experimental setup for local activation. The numbers indicated in the gel refer to the areas of which the absorbance or fluorescence intensity values are measured. Experimental data for areas 1–5 are reported in the following Figures.

vates a pathway for the hydrolysis of HPNPP through the cooperative action of neighboring $\text{TACN} \cdot \text{Zn}^{2+}$ -complexes.^[25] This implies that by activating a self-assembly process, HPNPP creates the conditions for its own destruction.^[26,27] In chemically fueled self-assembly this is an attractive property because the accelerated catalysis in the assembled state is a source of kinetic asymmetry, which is required to drive the system to a non-equilibrium composition.^[28,29] Regarding diffusion, we have recently shown that the local injection of a small amount of adenosine triphosphate (ATP) in the center of an agarose hydrogel containing surfactant $\text{C}_{12}\text{TACN} \cdot \text{Zn}^{2+}$ resulted in the local ATP-templated formation of assemblies with a very high thermodynamic stability.^[30] Since mass transport in hydrogels is regulated by diffusion and not convection, and since the assemblies are much larger than the free surfactants, local assembly formation caused the diffusion of free surfactant towards the center. Repetitive cycles of ATP-injection followed by spontaneous surfactant diffusion resulted in the gradual accumulation of assemblies in the center of the hydrogel. These results prompted us to investigate the dissipative self-assembly of $1_n \cdot \text{HPNPP}_m$ in agarose gel (Figure 1b).

Development of a macroscopic NESS. Agarose gels (1 mg ml^{-1} , buffered at pH 7.0) containing a homogeneous distribution of HPNPP ($100 \mu\text{M}$) were prepared in 6-well microtiter plates. A tiny volume ($1 \mu\text{L}$) of a concentrated stock solution of **1** (60 mM) was injected in the central position 1 of the gel and the absorbance at 405 nm was monitored with spatial resolution as a function of time (Figure 2b). Upon injection, we observed that, after an initial lag phase attributed to assembly formation, the absorbance in the center increased indicating the local formation of *p*-nitrophenolate (PNP, waste) from the assembly-catalysed hydrolysis of HPNPP (Figure 2b—black trace). The absorbance reached a maximum (after around 5 h, Figure 2b+2d-①), after which it very slowly decayed. Even after 15 h the absorbance in position 1 remained

significantly higher compared to other areas of the gel (Figure 2b+2e-②). The absorbance in positions 2–5 continued to gradually increase over the entire time interval as a result of PNP-diffusion from position 1 (Figure 2b). An important observation was made when plotting the overall conversion of HPNPP as a function of time (Figure 2c—red trace): the continuing increase in PNP concentration over the entire time interval revealed that the system remained catalytically active even after 19 h. The presence of catalytic activity was confirmed by the immediate decrease in absorbance in position 1 upon the injection of ATP, which is a strong competitive inhibitor of HPNPP hydrolysis (Figure 2b). Injection of ATP at a position remote from the center did not cause any change in absorbance (Figure S6).

Comparison of the overall catalytic performance with an equilibrated gel in which the same amounts of **1** and HPNPP were homogeneously distributed showed a remarkably higher activity for the non-equilibrium gel (Figure 2c+Figure S7). After 15 h the ongoing catalysis had already converted 30 % of HPNPP against just 8 % for the equilibrium gel.

Additional information on the catalytic activity in the gel was obtained by UPLC analysis of samples taken from positions 1 and 3, which permitted monitoring of both substrate and waste concentrations as a function of time (Figure 2f and Figure S5). The profiles of the PNP concentrations matched those obtained from absorbance measurements. On the other hand, the substrate concentration in position 1 drops relatively fast in the first 8 hours after which it stabilizes, whereas the substrate concentration in position 3 just shows a slow gradual decrease over the entire time interval. Interestingly, comparison of the sum of substrate and waste concentrations in position 1 and 3 showed an increase in position 1 compared to position 3, a difference that is maintained over time. This increase is attributed to the presence of assemblies that bind substrate and waste and therefore act as a local reservoir.

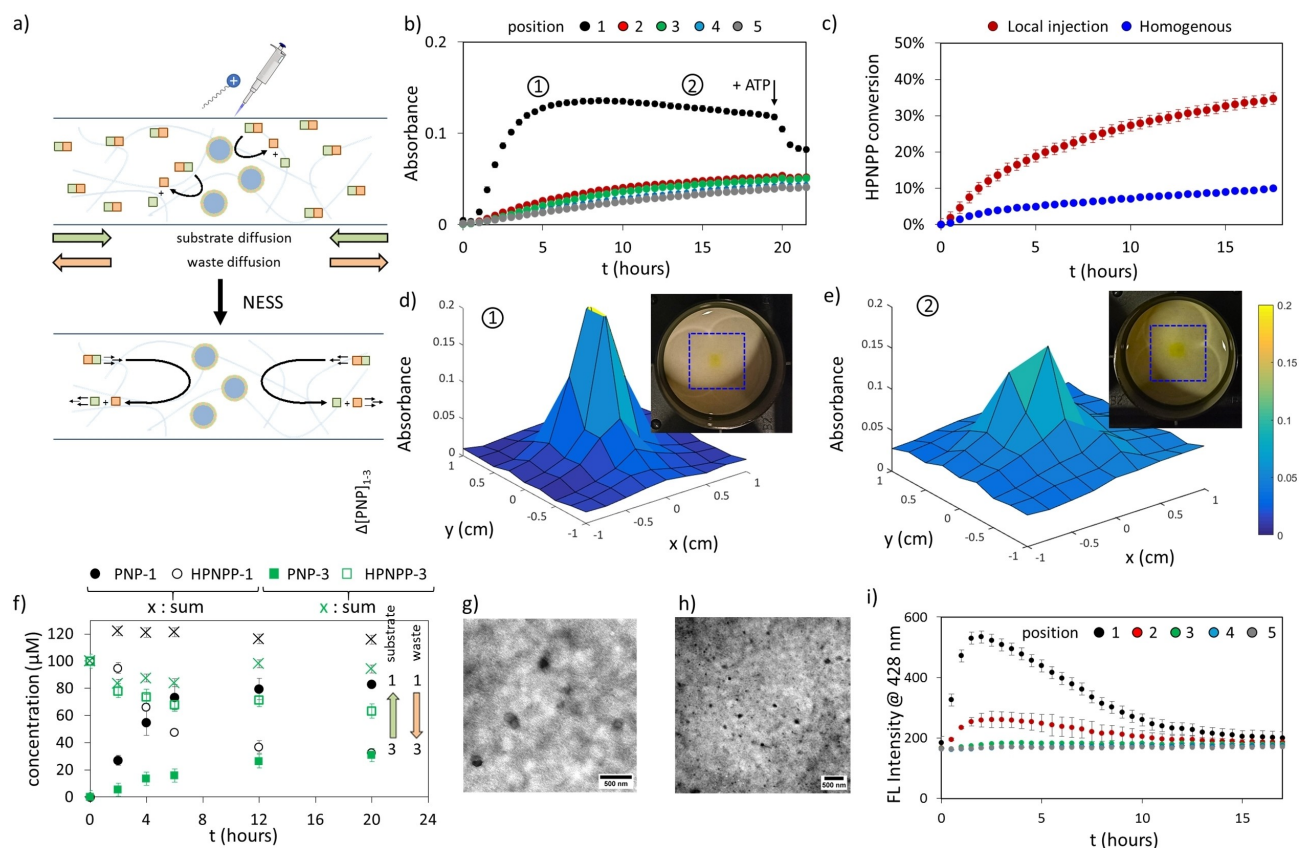


Figure 2. (a) Schematic representation of the processes that occur in a gel containing HPNPP upon the injection of **1**. b) Absorbance at 405 nm for positions 1–5 as a function of time after the injection of 1 μ L of a 60 mM stock solution of **1** in the center of a gel containing HPNPP (100 μ M). After 19 h, 1 μ L of a 5 mM stock solution of ATP was injected in the center. c) Plot of the HPNPP-conversion in the gel as a function of time for the gel in which HPNPP was injected (red trace) and for a control gel in which the same amount of HPNPP was homogeneously distributed (blue trace). d + e) 2D Contour plots of the absorbance at 405 nm of the gel at d) 5 h—①—and e) 15 h—②—after the injection of **1** in position 1. The insets are photographs of the gels with squares corresponding to the area of the 2D contour plots. f) Plot of the concentrations of substrate (open) and waste (filled) in positions 1 (black) and 3 (green) as a function of time as determined by UPLC: The asterisks indicate the sum of substrate and waste concentrations. The arrows indicate the direction of the concentration gradients for substrate and waste. g + h) Transmission electron microscopy (TEM) images of position 1 of the gel taken at time = 2 h (g) and 15 h (h). Additional TEM images are provided in section 9 of the Supporting Information. The scale bars correspond to 500 nm. i) Fluorescence intensity at 428 nm for positions 1–5 as a function of time after the injection of 1 μ L of a 60 mM stock solution of **1** in the center of a gel containing DPH (2.5 μ M), $\lambda_{\text{ex}}/\lambda_{\text{em}} = 355/428$, slits = 5/10. Experimental conditions: agarose = 1 mg/ml, [HEPES buffer] = 5 mM, $T = 25^\circ\text{C}$. Error bars indicate the standard deviation calculated from duplo measurements.

Confirmation that the catalytic activity was indeed linked to a substrate-induced self-assembly process was obtained by taking samples from the hydrogel for analysis by transmission electron microscopy (TEM). A sample taken from position 1 after 2 hours revealed the presence of assemblies with a diameter of around 180 ± 46 nm. The size is larger compared to those reported for the same system in a solution study,^[24] which is attributed to the presence of agarose.^[30] Importantly, assemblies were still clearly present after 15 h (Figure 2g, S9b) although with a slightly diminished size ($d \sim 90 \pm 39$ nm). A control sample taken from position 5 did not reveal any assemblies (Figure S12).

These data show that the injection of **1** in the HPNPP-containing gel results in the local formation of catalytically active assemblies $\mathbf{1}_n \cdot \text{HPNPP}_m$ that are sustained for very long times. After an initial phase of around 8 hours in which the formation of assemblies acts as a thermodynamic driving force for the diffusion of substrate to the center, a macro-

scopic non-equilibrium steady state (NESS) develops characterized by the local presence of energy dissipating assemblies and by substrate and waste concentration gradients that hardly vary over an extended period of time. The persistent concentration gradients are evidenced by the stable differences in both substrate and product concentrations in positions 1 and 3 (Figure 2f) for up to 20 hours. The approximately constant absorbance in position 1 indicates that the amount of PNP produced in position 1 through catalysis equals the amount of PNP diffusing from position 1 to 2. This implies that the amount of PNP that diffuses from position 1 to 2 is compensated by the same amount of HPNPP that diffuses from position 2 to 1. Although we use the term NESS it should be noted that the closed compartment of the gel implies that it would be more accurate to speak about a (pseudo-)NESS. Indeed, the catalytic activity and the concentration gradients gradually

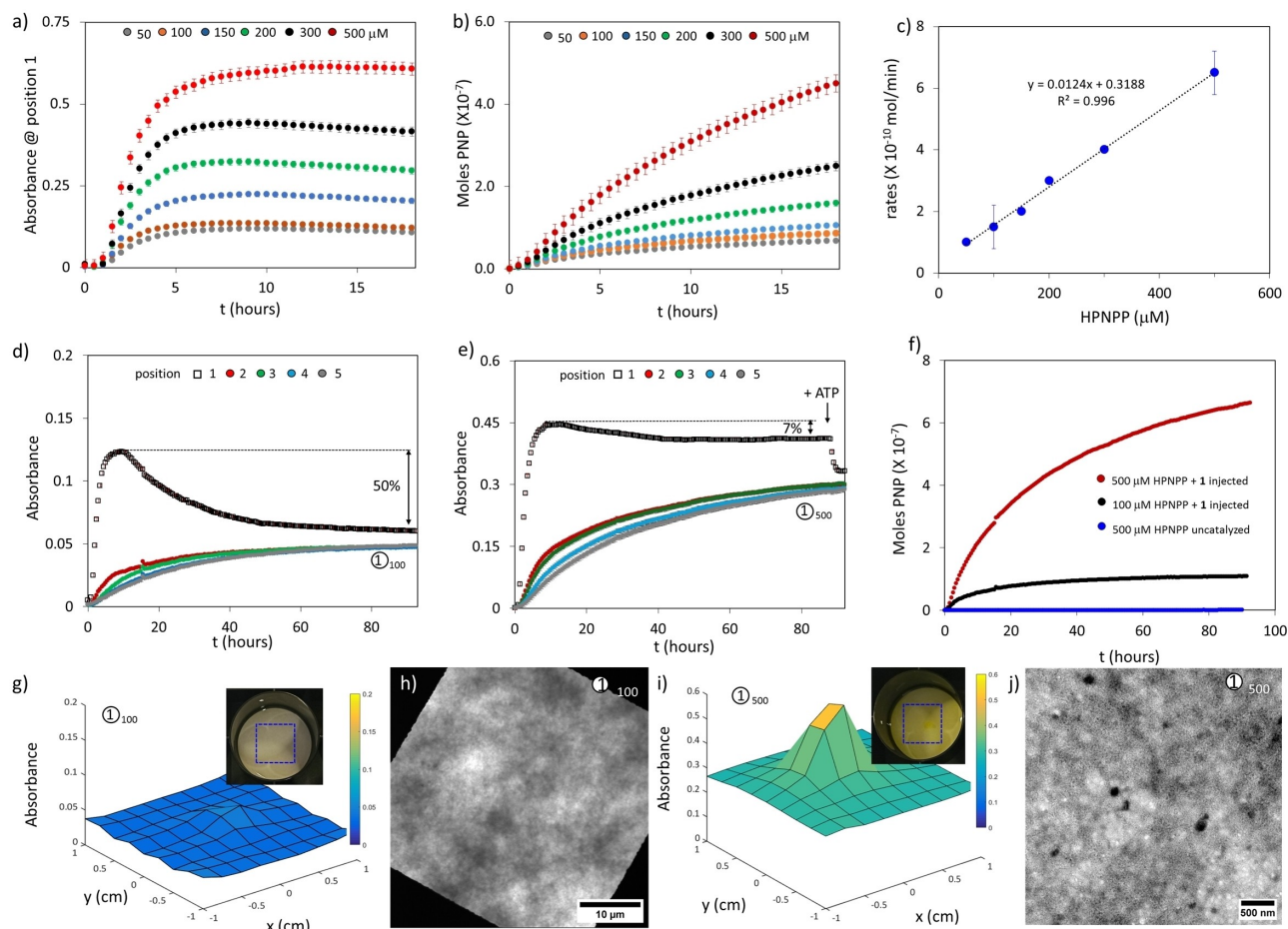


Figure 3. (a) Absorbance at 405 nm for position 1 as a function of time after the injection of 1 μ L of a 60 mM stock solution of **1** in the center of gels containing HPNPP ranging from 50–500 μ M. (b) Overall changes in the amount of PNP in gels as a function of time after the injection of **1** (1 μ L of a 60 mM stock solution) in position 1. (c) Initial rates of HPNPP hydrolysis ($t = 1$ h to 4.5 h) as a function of the initial amount of HPNPP present in the gel. The dotted line represents a fit to a straight line. (d) Absorbance at 405 nm for positions 1–5 as a function of time after the injection of 1 μ L of a 60 mM stock solution of **1** in the center of a gel containing HPNPP (100 μ M). (e) Absorbance at 405 nm for positions 1–5 as a function of time after the injection of 1 μ L of a 60 mM stock solution of **1** in the center of a gel containing HPNPP (500 μ M). After 88 h, 1 μ L of a 5 mM stock solution of ATP was injected in the center. (f) Overall changes in the number of moles of PNP in gels containing HPNPP (100 μ M and 500 μ M) as a function of time after the injection of **1** (1 μ L of a 60 mM stock solution) in position 1. In the control experiment (blue trace) surfactant was not injected in a gel containing 500 μ M HPNPP. (g) 2D Contour plot of the absorbance at 405 nm of the gel corresponding to $\textcircled{1}_{100}$ in 3d, the inset is a photograph of the gel with the square corresponding to the area of the 2D contour plot, at time = 80 h. (h) Transmission electron microscopy (TEM) image of position 1 of the gel taken at time = 100 h. The scale bar corresponds to 10 μ m. (i) 2D Contour plot of the absorbance at 405 nm of the gel corresponding to $\textcircled{1}_{500}$ in 3e, the inset is a photograph of the gel with the square corresponding to the area of the 2D contour plot, at time = 80 h. (j) Transmission electron microscopy (TEM) image of position 1 of the gel taken at time = 100 h. The scale bar corresponds to 500 nm. Additional TEM images are provided in section 9 of the Supporting Information. Experimental conditions: agarose = 1 mg/ml, [HEPES buffer] = 5 mM, $T = 25$ $^{\circ}$ C. Error bars indicate the standard deviation calculated from duplo measurements.

change over time because of a changing HPNPP:PNP ratio in the gel.

The presence of HPNPP in the gel is essential to sustain the existence of assemblies $\mathbf{1}_n\text{-HPNPP}_m$ in the center as evidenced by two control experiments. The system obtained by injecting **1** into a gel without HPNPP (using 1,6-diphenyl-1,3,5-hexatriene (DHP) as a fluorescent probe reporting on assembly formation)^[30] did not reach a steady state. Assemblies were initially present, but over time the assemblies disappeared as surfactant diffused away from the center and, after 15 h, the system had reached an equilibrium state (Figure 2i). In the second control experiment,

we injected HPNPP (1 μ L, 90 mM) into a gel containing **1** (100 μ M, Supporting Information, section 7). Upon injection, we observed an increase in absorbance in the center indicating the local formation of p-nitrophenolate (PNP). The absorbance reached a maximum after around 200 minutes after which it gradually decreased over time (Figure S8). After around 20 hours a stable situation was reached with a nearly homogeneous absorbance all over the gel. TEM analysis revealed that templated assemblies were no longer present (Figure S16).

The role of the substrate. The substrate HPNPP plays a critical role in the development and sustainment of the

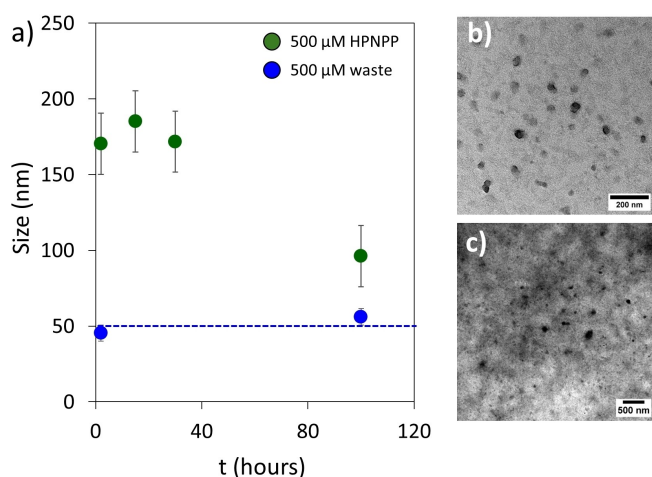


Figure 4. (a) Size distribution of structures as a function of time as observed in TEM images of gels containing 500 μM HPNPP (green) or 500 μM waste (blue) in which **1** was injected. TEM images of samples taken at $t=2$ h (b) and 100 h (c) from position 1 of a waste-containing gel (500 μM) in which 1 μL of a 60 mM stock solution of **1** was injected in the center. Additional TEM images are provided in Figure S14. The scale bars correspond to 200 and 500 nm, respectively. Error bars indicate the standard deviation.

macroscopic NESS because of its involvement in three processes: templated self-assembly, catalysis, and diffusion. To better understand the role of HPNPP, we studied the temporal evolution of gels with varying concentrations of HPNPP (50–500 μM) that were subjected to the injection of a constant amount of **1** (1 μL of a 60 mM stock solution, Figure 3a, S9). Analysis of the PNP-absorbance in position 1 revealed that an increase in the concentration of HPNPP had only a marginal effect on the time required to reach the stationary state (Figure S10), but that the stationary state absorbance in position 1 itself was proportionally related to the HPNPP concentration. All gels evolved to a NESS with a constant production of PNP, but at different rates (Figure 3b). This illustrates a higher catalytic activity in position 1 when higher HPNPP concentrations are present in the gel, even though the same amount of catalyst **1** was injected. The higher catalytic activity can be rationalized by considering the effect of increasing HPNPP concentrations on the equilibrium $n\mathbf{1} + m\text{HPNPP} \rightleftharpoons \mathbf{1}_n \cdot \text{HPNPP}_m$. From prior studies it is known that the affinity of HPNPP for multivalent TACN·Zn(II) surfaces is relatively low ($K_{\text{D,HPNPP}} \sim 1 \times 10^{-3}$ M).^[31,32] This implies that higher substrate concentrations shift the equilibrium towards the assembled state, which explains the higher catalytic activity. In the HPNPP concentration range studied it can be observed that the initial rate ($t=1$ h to 4.5 h after the lag phase) as a function of initial substrate concentration can be accurately fitted to a straight line (Figure 3c).

Apart from increasing the catalytic activity, the shift of the equilibrium towards the assembled state at higher substrate concentration has also a favorable effect on the lifetime of the dissipative assemblies. This property emerged from extended kinetic studies aimed at deciphering how long the NESS could be maintained. We repeated the

previously described experiment— injection of 1 μL of a 60 mM stock solution of **1** in a gel with 100 μM HPNPP— but now continued monitoring PNP-production for almost 4 days. It was observed that the gradual decrease in the absorbance at position 1, which to some extent was already evident in the shorter kinetic run (Figure 2b), continued and after four days a homogeneous gel was obtained that had become catalytically inactive (Figure 3d + f + g). TEM analysis of a sample taken at the end of the kinetics revealed that assemblies were no longer present (Figure 3h, Figure S9c). On the other hand, repetition of the experiment at 500 μM HPNPP concentration revealed that even after 4 days, the absorbance in position 1 remained significantly higher compared to the other positions with just a minor decrease ($\sim 7\%$) compared to the maximum at $t=8$ h (Figure 3e + i). After 4 days catalytic activity was still occurring in the gel, evidenced by the continuing overall increase in PNP concentration (Figure 3f—red trace) and the observed drop in local absorbance upon the injection of ATP (Figure 3e). Also, TEM analysis confirmed that after 4 days ($t=100$ h) assemblies (Figure 3j, Figure S13) were still present in position 1 although the dimensions ($d \sim 96 \pm 32$ nm) had decreased compared to those present in a sample taken after 15 hours ($d \sim 185 \pm 61$ nm) (see also Figure 4a). The increased lifetime of the assemblies in the center of the gel at 500 μM substrate concentrations can be explained considering the higher thermodynamic stability of the assemblies. In other words, high substrate concentrations slow down ‘leakage’ of **1** from assemblies $\mathbf{1}_n \cdot \text{HPNPP}_m$ and this slows down diffusion of **1** to other areas of the gel.

Even though at 500 μM substrate concentrations assemblies persisted in the center of the gel, their size gradually decreased over time (Figure 4a). This decrease is attributed to a gradual depletion of substrate in the system. Information on the ‘thermodynamic endpoint’ of the system was obtained by injecting **1** in the center of a gel containing the waste mixture (500 μM of fully hydrolyzed HPNPP) and sampling the assembly size at $t=2$ h and 100 h. Coherent with the known templating ability of waste,^[24] assemblies also persisted in this gel for a long time, but the waste-stabilized assemblies were significantly smaller in size ($d = 50 \pm 10$ nm) and, importantly, their size did not change over time (Figure 4a–c, Figure S14). Altogether, these studies reveal that local formation of a dissipative structure and substrate/waste-concentration gradients is interdependent. The effect of the dissipative self-assembly process on the concentration gradients is clear: substrate and waste concentration gradients do not emerge in the absence of catalysis. Reversely, the continuous diffusion of the substrate towards the assemblies enables the latter to maintain a large size.

A reaction-diffusion model. Despite the complexity of the processes that are activated when surfactants are injected in the gel, we were interested whether a minimalistic reaction-diffusion model could be built to qualitatively support our interpretation of the experimental data. The model is described in detail in the Supporting Information; here we only give a concise presentation. In the model we assume that the assemblies form in a fast initial phase after the injection of the stock solution; the ‘time-zero’ corre-

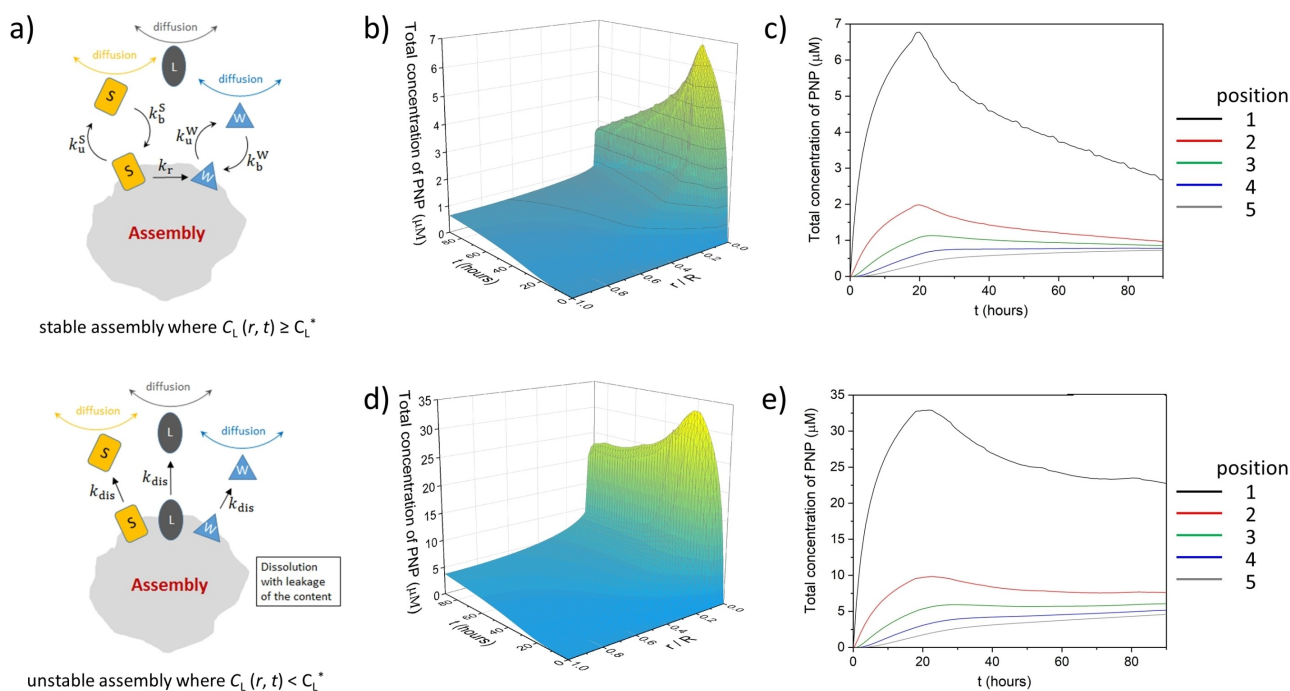


Figure 5. (a) Schematic representation of the processes included in the minimal reaction-diffusion model and relevant kinetic parameters. Dissolution of the assemblies is modeled by assuming that leakage of compounds (free PNP plus PNP in the assemblies) will start once the concentration of free surfactants falls below a threshold concentration. (b) Calculated profiles of the PNP total concentration (free PNP plus PNP in the assemblies) versus time and radial distance from the center of the reaction well. Panels (b) and (c) refer to the HPNPP initial concentration 100 μM ('Case 1' below) while panels (d) and (e) refer to 500 μM ('Case 2' below). Panels (b) and (d) show the full profile while panels (c) and (e) report the time evolution at the five sampling distances of the experiments. The profiles were obtained from a minimal reaction-diffusion model (details are provided in the Supporting Information). In all cases, the binding/unbinding rate constants were set equal to $5 \times 10^{-3} \text{ s}^{-1}$. The dissolution rate constant were set equal to $5 \times 10^{-4} \text{ s}^{-1}$ in Case 1 and to 10^{-4} s^{-1} in Case 2. The diffusion coefficient of each species was set equal to $5 \times 10^{-10} \text{ m}^2 \text{ s}^{-1}$. The fraction of assembled surfactants (ϕ) was set equal to 0.3 in Case 1 and 0.5 in Case 2. The threshold concentration (C_L^*) was set to 34 μM in Case 1 and 24 μM in Case 2. The dimensions of the reaction well are the experimental ones (radius 1.745 cm, depth 3.1 mm) and the injected surfactants correspond to 1 μL of the 60 mM stock solution. The assemblies are assumed to initially have a bell-shaped distribution that drops to zero at the distance R^* of about 1.45 mm in both Case 1 and Case 2; the concentration of free surfactants is depleted accordingly. The rate constant of the HPNPP reaction was taken equal to $7.1 \times 10^{-6} \text{ s}^{-1}$. The numerical solution was obtained by means of a finite-difference scheme. The irregular features of the profiles are due to the dynamical discontinuities that are present in the model (see the Supporting Information).

sponds to the end of that phase. The parameter ϕ defines the ratio of **1** in the free and assembled form. The radial distribution of the assemblies around the injection point is taken to have a bell-shaped profile, and beyond a distance R^* no assemblies are present. Then, the substrate HPNPP (label **S**) and the waste product PNP (label **W**) can bind/unbind to/from the assemblies with given first-order rate constants; the 'neutral' binding/unbinding of the surfactant **1** (label **L**) is ignored as long as the assemblies are structurally stable. The irreversible reaction of **S** to **W** is assumed to take place only in/on the assemblies with a given first-order rate constant. All species **S**, **W** and **L** are free to diffuse in the gel phase. It is assumed that the assemblies become unstable when the local concentration of free **L** drops below a threshold value C_L^* ; when this happens, it is assumed that **S** and **W** stop binding to the assemblies which start dissolving with a first-order process of given rate constant k_{dis} . During the dissolution, the assemblies release their content of **S**, **W** and **L** into the solution. It is likely to assume that ϕ increases, while both C_L^* and k_{dis} decrease as the initial concentration of the substrate is higher and higher.

This is because HPNPP promotes the formation of the assemblies and stabilize them both from the thermodynamic and kinetic point of view. The initial conditions at time-zero are of **S** homogeneously distributed (assuming that the fraction of **S** incorporated in the assemblies is negligible), **W** absent, and both free and assembled **L** distributed with a bell-shaped distribution (which sharply drops to zero at a distance R^* for the assembled surfactants). With such a setup, the reaction-diffusion partial derivative equations were elaborated and numerically solved by means of a finite-difference scheme (see Supporting Information section 11 for details).

Figure 5 shows the outcomes for a set of kinetic parameters tuned to achieve a qualitative agreement with the experimental profiles. Figures 5b and 5d show the total concentration of PNP (free and in the assemblies), versus the time and the distance from the center, for the initial substrate concentration 100 μM and 500 μM . Figures 5c and 5e report the evolution of the total concentration of PNP at the five sampling positions of the experiments. We can see that these profiles are qualitatively close to the experimental

trends of the absorbance (Figures 3d and 3e). Concerning the profiles that refer to position 1 (center of the reaction well), the initial growth is due to the binding of the substrate to the assemblies, with consequent conversion into waste. The maximum of the profile corresponds to the turning point when the local concentration of free **L** drops below the threshold value (because of diffusion of surfactants from the center towards the periphery). This implies that the assemblies start to dissolve and, in turn, this causes the progressive reduction of PNP production. As the produced PNP diffuses towards the periphery, its concentration at the center decreases while the concentration at the sampling positions 2, 3, 4 and 5 grows. In the very long timescale, not reached in these simulations, the profiles for all positions converge because all assemblies eventually dissolve and the concentration of PNP tends to be uniform. In short, the parameters that mainly control the evolution of the concentration in the central position are the fraction ϕ , the threshold concentration C_L^* which affects the turning point on the time axis and, crucially, the rate constant of dissolution k_{dis} which controls the persistence of the pseudo-stationary state during which the substrate continues to react in the assemblies while they slowly dissolve. We can also see that the increase of ϕ and the decrease of C_L^* and k_{dis} , which likely accompany the increase of initial substrate concentration, produce a more persistent pseudo-stationary state at position 1 with a smaller drop after the turning point at the maximum. This is in accord with the experimental finding.

Conclusion

In conclusion, we have shown that the local activation of a dissipative self-assembly process in a macroscopic gel containing substrate results in the formation of a macroscopic (pseudo-)stationary non-equilibrium state. This state is characterized by the local presence of energy dissipating assemblies and persistent substrate and waste concentration gradients. The opposing concentration gradients of substrate and waste ensure that the spatially confined assemblies experience (semi-)chemostatted conditions that persist for elongated periods. Our studies reveal an interdependence between the energy-dissipating structures and the substrate/waste concentration gradients. The importance of such an interdependence between catalysis and concentration gradients for developing macroscopic non-equilibrium properties was recently demonstrated.^[33] The straightforward approach to study dissipative structures under (semi-)chemostatted conditions will facilitate the study of properties originating from the non-equilibrium state of energy-dissipating structures. The development of reaction-diffusion models that accurately provide a qualitative and quantitative description will benefit from the use of simple dissipative systems of which all processes are fully understood at the molecular level. Finally, the introduction of space as a dimension in the study of dissipative self-assembly processes is crucial for our understanding how energy-dissipating processes at the molecular level can be transposed to a

macroscopic dimension, which is essential for the development of synthetic active matter.^[20,21]

Supporting Information

Procedures, experimental details and supporting data is available. The authors have cited additional references within the Supporting Information.

Acknowledgements

This work was financially supported by the Italian Ministry of Education and Research (L.J.P., grant 2022TSB8P7 and P2022ANCEK) and the University of Padova (L.J.P., grant P-DiSC #CASA-BIRD2022-UNIPD). HK thanks the MUR for a Young Researchers, Seal of Excellence fellowship (PNRR) funded by the European Union—NextGeneration EU.

Conflict of Interest

The authors declare no conflict of interest.

Data Availability Statement

The data that support the findings of this study are available from the corresponding author upon reasonable request.

Keywords: dissipative self-assembly · reaction-diffusion · systems chemistry · non-equilibrium · hydrogel

- [1] B. A. Grzybowski, W. T. S. Huck, *Nat. Nanotechnol.* **2016**, *11*, 585–592.
- [2] G. Ashkenasy, T. M. Hermans, S. Otto, A. F. Taylor, *Chem. Soc. Rev.* **2017**, *46*, 2543–2554.
- [3] R. Merindol, A. Walther, *Chem. Soc. Rev.* **2017**, *46*, 5588–5619.
- [4] B. Rieβ, R. K. Grötsch, J. Boekhoven, *Chem* **2020**, *6*, 552–578.
- [5] N. Singh, G. J. M. Formon, S. De Piccoli, T. M. Hermans, *Adv. Mater.* **2020**, *32*, 1906834.
- [6] K. Das, L. Gabrielli, L. J. Prins, *Angew. Chem. Int. Ed.* **2021**, *60*, 20120–20143.
- [7] T. Mitchison, M. Kirschner, *Nature* **1984**, *312*, 237–242.
- [8] A. Desai, T. J. Mitchison, *Annu. Rev. Cell Dev. Biol.* **1997**, *13*, 83–117.
- [9] H. Hess, J. L. Ross, *Chem. Soc. Rev.* **2017**, *46*, 5570–5587.
- [10] J. Boekhoven, W. E. Hendriksen, G. J. M. Koper, R. Eelkema, J. H. van Esch, *Science* **2015**, *349*, 1075–1079.
- [11] J. Leira-Iglesias, A. Tassoni, T. Adachi, M. Stich, T. M. Hermans, *Nat. Nanotechnol.* **2018**, *13*, 1021–1027.
- [12] M. G. Howlett, A. H. J. Engwerda, R. J. H. Scanes, S. P. Fletcher, *Nat. Chem.* **2022**, *14*, 805–810.
- [13] P. Bastiaens, M. Caudron, P. Niethammer, E. Karsenti, *Trends Cell Biol.* **2006**, *16*, 125–134.
- [14] R. Wollman, E. N. Cytrynbaum, J. T. Jones, T. Meyer, J. M. Scholey, A. Mogilner, *Curr. Biol.* **2005**, *15*, 828–832.
- [15] A. van der Weijden, M. Winkens, S. M. C. Schoenmakers, W. T. S. Huck, P. A. Korevaar, *Nat. Commun.* **2020**, *11*, 1–10.

- [16] H. Fu, N. Cao, W. Zeng, M. Liao, S. Yao, J. Zhou, W. Zhang, *J. Am. Chem. Soc.* **2024**, *146*, 3323–3330.
- [17] A. M. Bergmann, J. Bauermann, G. Bartolucci, C. Donau, M. Stasi, A. L. Holtmannspötter, F. Jülicher, C. A. Weber, J. Boekhoven, *Nat. Commun.* **2023**, *14*, DOI 10.1038/s41467-023-42344-w.
- [18] C. Donau, F. Späth, M. Sosson, B. A. K. Kriebisch, F. Schnitter, M. Tena-Solsona, H. S. Kang, E. Salibi, M. Sattler, H. Mutschler, J. Boekhoven, *Nat. Commun.* **2020**, *11*, 5167.
- [19] E. te Brinke, J. Groen, A. Herrmann, H. A. Heus, G. Rivas, E. Spruijt, W. T. S. Huck, *Nat. Nanotechnol.* **2018**, *13*, 849–855.
- [20] O. E. Shklyae, A. C. Balazs, *Nat. Nanotechnol.* **2024**, *19*, 146–159.
- [21] A.-D. C. Nguindjel, P. J. de Visser, M. Winkens, P. A. Korevaar, *Phys. Chem. Chem. Phys.* **2022**, 23980–24001.
- [22] G. Fusi, D. Del Giudice, O. Skarsetz, S. Di Stefano, A. Walther, *Adv. Mater.* **2023**, *35*, 2209870.
- [23] A. Sorrenti, J. Leira-Iglesias, A. Sato, T. M. Hermans, *Nat. Commun.* **2017**, *8*, 15899.
- [24] P. Solís Muñana, G. Ragazzon, J. Dupont, C. Z.-J. Ren, L. J. Prins, J. L.-Y. Chen, *Angew. Chem.* **2018**, *57*, 16469–16474.
- [25] L. J. Prins, F. Mancin, P. Scrimin, *Curr. Org. Chem.* **2009**, *13*, 1050–1064.
- [26] S. Bal, K. Das, S. Ahmed, D. Das, *Angew. Chem. Int. Ed.* **2019**, *58*, 244–247.
- [27] S. P. Afrose, C. Ghosh, D. Das, *Chem. Sci.* **2021**, *12*, 14674–14685.
- [28] G. Ragazzon, L. J. Prins, *Nat. Nanotechnol.* **2018**, *13*, 882–889.
- [29] R. D. Astumian, *Nat. Commun.* **2019**, *10*, 3837.
- [30] R. Chen, K. Das, M. A. Cardona, L. Gabrielli, L. J. Prins, *J. Am. Chem. Soc.* **2022**, *144*, 2010–2018.
- [31] R. Bonomi, A. Cazzolaro, A. Sansone, P. Scrimin, L. J. Prins, *Angew. Chem. Int. Ed.* **2011**, *50*, 2307–2312.
- [32] C. Pezzato, L. J. Prins, *Nat. Commun.* **2015**, *6*, 7790.
- [33] N. S. Mandal, A. Sen, R. D. Astumian, *Chem* **2024**, *10*, 1147–1159.

Manuscript received: March 6, 2024

Accepted manuscript online: May 8, 2024

Version of record online: June 21, 2024